Detection of Exudates in Fundus Images Using a Markovian Segmentation Model

Balazs Harangi – *IEEE member*, Andras Hajdu – *IEEE member*

Abstract— **Diabetic retinopathy (DR) is one of the most common causing of vision loss in developed countries. In early stage of DR, some signs like exudates appear in the retinal images. An automatic screening system must be capable to detect these signs properly so that the treatment of the patients may begin in time. The appearance of exudates shows a rich variety regarding their shape and size making automatic detection more challenging. We propose a way for the automatic segmentation of exudates consisting of a candidate extraction step followed by exact contour detection and region-wise classification. More specifically, we extract possible exudate candidates using grayscale morphology and their proper shape is determined by a Markovian segmentation model considering edge information. Finally, we label the candidates as true or false ones by an optimally adjusted SVM classifier. For testing purposes, we considered the publicly available database DiaretDB1, where the proposed method outperformed several state-of-the-art exudate detectors.**

I. Introduction

More than 360 million people suffer worldwide from diabetes in 2013 which disease is expected to be the seventh leading cause of death by 2030 according to World Health Organization (WHO) [1]. Diabetes also causes damage to the retina of patients suffering from for 10 years or more, which disease is known as diabetic retinopathy (DR). Currently, DR is the leading reason of blindness. Despite of these frightening facts, 90% of the new cases can be cured if the patients got proper treatment in time. Because of the growing tendency of DR, automatic screening systems which can detect its first signs has great importance mainly in developed countries, where near 40% of the cases remain undiagnosed.

Exudates are among the first signs of DR and arise, when fluid exudes from tissue due to injured capillaries. These lesions have yellowish, bright color and various sizes with irregular shapes, as can be seen in Figure 1. This appearance makes automatic exudate detection difficult.

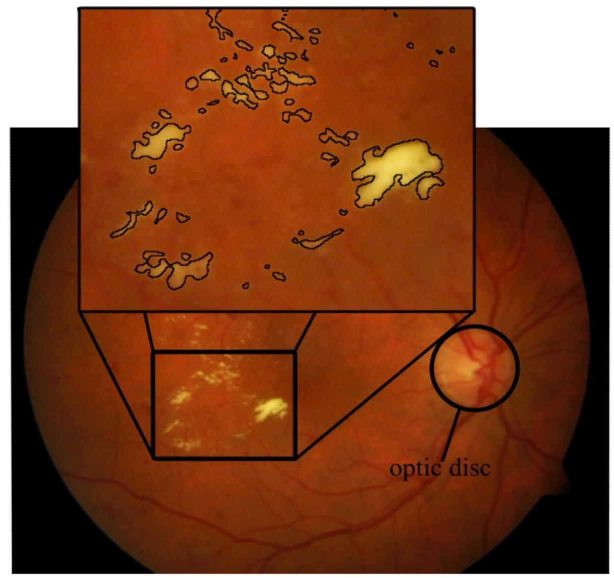

Figure 1. Exudates appear as yellowish, bright patches of various size and irregular shape.

We can find several exudate detection algorithms in the literature that can be divided into two main categories. The first group consists of algorithms based on grayscale morphology [2], [3], [4], while other approaches are based on pixel-wise classification [5], [6], [7]. Some methods [8] fall out of these groups. Morphology based algorithms sometimes detect the bright regions of the fundus images wrongly as exudates. Moreover, the pixel-wise labeling of the images takes too much time. In this paper, we propose an approach, which can segment and detect exudates on RGB fundus images. This method uses grayscale morphology for candidate extraction and initialization of a Markovian segmentation model to detect quickly the contours of the candidates. Finally, we classify only the candidates as true or false ones based on some region-wise features. The workflow of our approach can be observed in Figure 2.

The rest of the paper is organized as follows: in section 2, we describe our candidate extraction step using morphological operators. Section 3 is devoted for the extraction of the boundaries by Markovian segmentation. The region-wise labeling approach is given in section 4. In

* This work was partly supported by the project DRSCREEN – Developing a computer based image processing system for diabetic retinopathy screening of the National Office for Research and Technology of Hungary (contract no.: OM-00194/2008, OM-00195/2008, OM-00196/2008) and by the European Union and the State of Hungary, co-financed by the European Social Fund in the framework of TÁMOP-4.2.4.A/ 2-11/1-2012-0001 'National Excellence Program'.

B. Harangi, A. Hajdu are with the Faculty of Informatics, University of Debrecen, Debrecen, 4010 POB. 12, Hungary (e-mail: {harangi.balazs,hajdu.andras}@inf.unideb.hu).

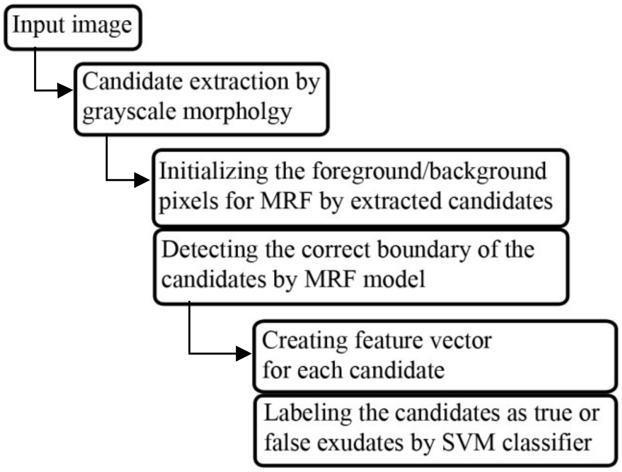

Figure 2. The workflow of our approach.

section 5, we present our experimental results and finally, some conclusions are drawn in section 6.

II. Candidate extraction

In this section, we give a brief overview about the applied candidate extraction method. Then, in a later section, we demonstrate how we can use these candidates as an initial set of pixels of foreground and background for Markov Random Fields to construct a segmentation model.

Walter et al. [2] proposed an exudate segmentation method using grayscale morphology operators. Namely, high local contrast and intensities as the most typical features of exudates are considered. The vascular system is eliminated through a grayscale morphological closing. Then, in the vessel-free image, local variation is calculated at each pixel using its local neighborhood. The regions with low local variation are also eliminated. Next, to exclude the darker regions and to extract bright objects, thresholding is applied for the remaining regions. To refine the shape of a candidate, morphological reconstruction is used and the result is subtracted from the original image. Since this algorithm considers bright regions with high contrast, the result $\boldsymbol{I_{BW}}$ contains false candidates for young patients, when a shining elongated regions spread along the temporal arcade as can be seen in Figure 3. Moreover, the shapes of the candidates are not accurate due to the applied structuring elements. To overcome these deficiencies, we will propose a Markovian segmentation model and a region-wise labeling.

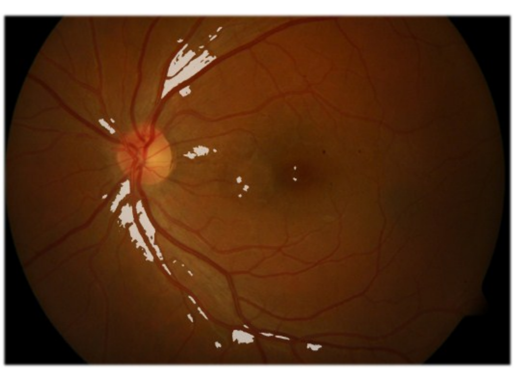

Figure 3. Marked by white the result of candidate extraction.

III. Precise contour detection by a Markovian segmentation model

Markov Random Field (MRF) provides a robust tool to find exact boundaries of exudates by minimizing a specific energy function. To find the global minimum for the usual energy function is an *NP*-hard problem, however, certain energy functions can be minimized in polynomial time by graph cuts. Lesko et al. [9] proposed a segmentation algorithm, which requires user interaction to mark an initial set of foreground/background pixels. Then, segmentation is performed via graph cut in real time.

Now we give a brief overview of the novel MRF model proposed by Lesko et al. As a well-known approach, segmentation can be considered as a labeling problem, where we assign labels $\boldsymbol{\omega_s} \in \{\boldsymbol{0}, \boldsymbol{1}\}, \boldsymbol{s} \in \boldsymbol{S}$ to the pixels $\boldsymbol{S} = \{\boldsymbol{s_1}, \dots, \boldsymbol{s_N}\} \subset \mathbb{Z}^2$ based on some observed features $\boldsymbol{\mathcal{F}} = \{\boldsymbol{f_s}\}$ of them. Based on the Bayesian theorem, the posterior probability can be factorized as $\boldsymbol{P(\omega|\mathcal{F}) \propto P(\mathcal{F}|\omega)P(\omega)}$, where the optimal segmentation $\boldsymbol{\hat{\omega}}$ is obtained as the *Maximum a Posteriori* (MAP) estimate. Based on the *Hammersley-Clifford* theorem [10], $\boldsymbol{\hat{\omega}}$ can be found with specifying MRF with clique potentials and minimizing Gibbs energy. The main contribution of [9] is to construct the Gibbs energy function in a way that it can be minimized via standard max-flow/min-cut. Namely, the full gradient information is exploited as magnitude and direction next to the gray-level intensity and only the pairwise interactions (doubleton cliques) are considered. In this way, the constructed Gibbs energy can be represented by a graph and an exact MAP solution can be determined by computing the minimum *s-t-cut* on the graph [11] in polynomial time.

For the precise segmentation of the candidates, we apply this optimized MRF model with a modification to make the method automatic. So to eliminate user interaction, we define the initial foreground/background pixels as the result of candidate extraction $\boldsymbol{I_{BW}}$. Based on our experiments, the MRF model provides the most precise boundaries of candidates, when the foreground pixels are defined by $\boldsymbol{I_{BW}}$ after applying morphological opening with a structuring element of size *3 x 3* pixels. For the assignment of the background pixels, we invert $\boldsymbol{I_{BW}}$ and perform an opening operation with a structuring element of size *7 x 7* pixels. The result $\boldsymbol{I_{aMRF}}$ of the MRF model initialized automatically can be seen in Figure 4.

IV. Regionwise classification

In this section, we explain our proposed post-processing step, where we eliminate the false exudate candidates to enhance the specificity of the algorithm. As an initial step, to compensate the similarities between the optic disc (OD) and exudates, we eliminate the candidates falling in the region of the OD using the detection algorithm [12].

To label the remaining candidates as true or false ones, we collect certain features for each candidate and apply an SVM supervised classifier. For feature extraction, we consider the green intensity channel $\boldsymbol{I_G}$ of the RGB fundus image, since it contains the most information about the lesions and anatomical parts of the retina. Moreover, to enhance the local contrast of exudates, we apply a contrast-

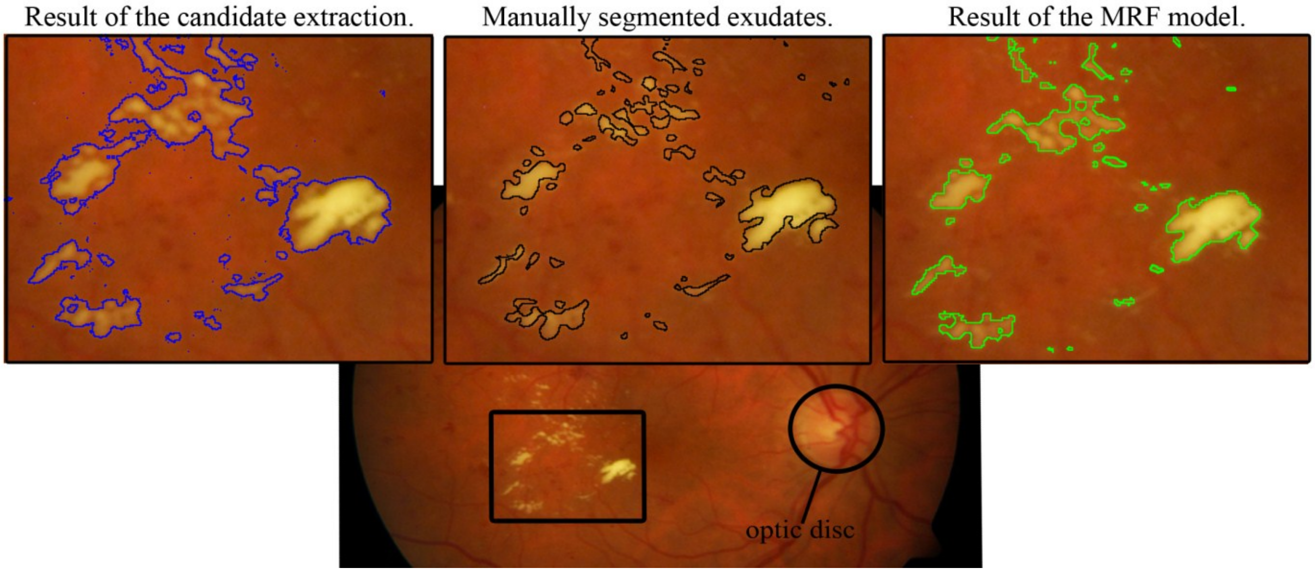

Figure 4. Result of the precise contour detection.

limited adaptive histogram equalization on $\boldsymbol{I_G}$ to obtain $\boldsymbol{I_{CLAHE}}$. To construct a feature vector for a candidate, we extract some intensity based statistical descriptors from the pixels composing the candidate using $\boldsymbol{I_G}$ and $\boldsymbol{I_{CLAHE}}$. We also extract some shape descriptors from the precisely detected candidate region. The whole list of these features is enclosed in Table 1.

TABLE I. COMPONENTS OF THE FEATURE VECTOR FOR REGION-WISE CLASSIFICATION.

Extracted From	Name of the Descriptor
pixel intensities of I_G belonging to the candidate	-mean -standard deviation -maximum value
pixel intensities of I_{CLAHE} belonging to the candidate	-mean -standard deviation -maximum value
shape of the candidate region	- compactness - area - number of holes - elongatedness - eccentricity - perimeter

In the training phase of SVM classification, we have performed candidate extraction on the training images and applied the MRF model to them. Next, each of the extracted candidates on $\boldsymbol{I_{aMRF}}$ has been marked manually as true or false exudates by a local ophthalmologist. In this way, we have gathered a set of true and false candidates for training the SVM. To create the training dataset, the feature vector (see Table 1) is extracted from each candidate and a label is assigned to the vector based on the manual annotation.

In the decision phase, for an input fundus image $\boldsymbol{I}$ we apply candidate extraction and initialize the MRF model with its result $\boldsymbol{I_{BW}}$ to determine the precise boundary of the candidates. Finally, we label each candidate in $\boldsymbol{I_{aMRF}}$ as true/false by an SVM classifier to eliminate the false ones.

V. EXPERIMENTAL RESULTS

We have evaluated the performance of our approach on the DIARETDB1 – Standard Diabetic Retinopathy Database [13]. DIARETDB1 contains 89 fundus images with a 50° field-of-view and resolution of 1500×1152 pixels. Within this database, 53 images contain exudates and their most representative points are also given. Based on these reference exudates points, a local ophthalmologist has segmented manually the lesions for each database image, and created a binary mask $\mathbf{I_{manual}}$ with their precise boundaries.

To test the performance of our approach, we consider the *F*-Score measure (1). *F*-Score can be interpreted as a weighted average of sensitivity (2) and positive predictive value (*PPV*) (3). The true positive (*TP*), false positive (*FP*) and false negative (*FN*) figures are considered at pixel level.

$$\mathbf{F\text{–}Score} = \frac{\mathbf{2 \cdot Sensitivity \cdot PPV}}{\mathbf{Sensitivity + PPV}}, \tag{1}$$

$$\mathbf{Sensitivity} = \frac{\mathbf{TP}}{\mathbf{TP + FN}}, \tag{2}$$

$$\mathbf{PPV} = \frac{\mathbf{TP}}{\mathbf{TP + FP}}. \tag{3}$$

As a comparative study, Table 2 shows the performance of the proposed method and some re-implemented state-of-the-art algorithms [2-8] regarding their *F*-Score on the dataset DiaretDB1. Note that the algorithms [5-8] are not optimized for precise (pixel level) exudate detection that explains their low *F*-Score figures in this study.

We have evaluated our approach at image level, as well. In this case, *TP* stands for the number of images containing exudates according to both $\mathbf{I_{manual}}$ and $\mathbf{I_{res}}$. Similarly, *FP* holds the number of images containing exudates according to $\mathbf{I_{res}}$ only, while *FN* denotes the number of images with the

TABLE II. COMPARATIVE RESULTS FOR PRECISE (PIXEL LEVEL) EXUDATE DETECTION.

	F-Score	*Sensitivity*	*PPV*
Proposed method	0.71	0.73	0.69
Walter [2]	0.67	0.76	0.59
Sopharak [3]	0.56	0.40	0.91
Welfer [4]	0.31	0.19	0.92
Jaafar [8]	0.17	0.89	0.09
Sopharak [5]	0.16	0.49	0.09
Sopharak [6]	0.11	0.82	0.06
Sánchez [7]	0.15	0.38	0.10

reversed setup. As we can see from Table 3, the proposed algorithm outperformed the state-of-the-art algorithms [2-8] at image level, as well.

TABLE III. COMPARATIVE RESULTS AT IMAGE LEVEL.

	F-Score	*Sensitivity*	*PPV*
Proposed method	0.81	0.90	0.73
Sopharak [3]	0.80	0.73	0.89
Sopharak [5]	0.77	1.00	0.62
Sánchez [7]	0.77	0.66	0.92
Walter [2]	0.75	1.00	0.60
Welfer [4]	0.75	0.79	0.71
Sopharak [6]	0.75	1.00	0.59
Jaafar [8]	0.75	1.00	0.60

VI. CONCLUSION

In this paper, we have proposed an approach for automatic exudate segmentation. Our method starts with candidate extraction using grayscale morphology operators. Based on the candidates, we apply a Markovian segmentation model to detect the precise boundaries of the candidates. Finally, as a post-processing step, we exclude false candidates with a supervised SVM classifier. In an experimental study on a publicly available database, we have found that our approach achieved higher F-Score figure in comparison with several state-of-the-art approaches at both pixel and image levels. Our approach was implemented in Matlab R2010b (Bioinformatics, Image Processing and Statistics Toolboxes), and we used a single core 2,4GHz CPU with 2GB memory for testing and the average computational time is below 10 seconds per image.

ACKNOWLEDGMENT

The authors thank Zoltán Kató for his support regarding the implementation of the applied MRF model.

REFERENCES

[1] J. E. Shaw, R. A. Sicree, and P. Z. Zimmet, “Global estimates of the prevalence of diabetes for 2010 and 2030”, *Diabetes Research and Clinical Practice*, vol. 87, no. 1, pp. 4-14, 2010.

[2] T. Walter, J. C. Klein, P. Massin and A. Erginay, ”A contribution of image processing to the diagnosis of diabetic retinopathy – detection of exudates in color fundus images of the human retina”, *IEEE Transactions on Medical Imaging*, vol. 21, no. 10, pp. 1236–43, 2002.

[3] A. Sopharak, B. Uyyanonvara S. Barman and T. H. Williamson, ”Automatic detection of diabetic retinopathy exudates from non-dilated retinal images using mathematical morphology methods”, Computerized Medical Imaging and Graphics, vol. 32, no. 8, pp. 720–727, 2008.

[4] D. Welfer, J. Scharcanski and D. R. Marinho, ”A coarse-to-fine strategy for automatically detecting exudates in color eye fundus images”, Computerized Medical Imaging and Graphics, vol. 34, no. 3, pp. 228–235, 2010.

[5] A. Sopharak, B. Uyyanonvara and S. Barman, ”Automatic exudate detection from nondilated diabetic retinopathy retinal images using fuzzy c-means clustering”, Sensors, vol. 9, no. 3, pp. 2148–2161, 2009.

[6] A. Sopharak, M. N. Dailey, B. Uyyanonvara, S. Barman, T. Williamson, K. T. Nwe and Y. A. Moe, ”Machine learning approach to automatic exudate detection in retinal images from diabetic patients”, Journal of Modern Optics, vol. 57, no. 2, pp. 124-135, 2010.

[7] C. I. Sánchez, R. Hornero, M. I. López, M. Aboy, J. Poza and D. Abásolo, ”A novel automatic image processing algorithm for detection of hard exudates based on retinal image analysis”, Medical Engineering & Physics, vol. 30, no. 3, pp. 350-357, 2008.

[8] H. F. Jaafar, A. K. Nandi and W. Al-Nuaimy, “Detection of exudates in retinal images using a pure splitting technique”, Engineering in Medicine and Biology Society, pp. 6745-6748, 2010.

[9] M. Lesko, Z. Kato, A. Nagy, I. Gombos, Zs. Török, L. Vígh Jr. and L. Vígh, “Live Cell Segmentation in Fluorescence Microscopy via Graph Cut”, In Proceedings of International Conference on Pattern Recognition (ICPR), Istambul, Turkey, pp. 1485-1488, 2010.

[10] S. Geman and D. Geman, “Stochastic relaxation, Gibbs distributions, and the Bayesian restoration of images,” IEEE Transactions on Pattern Analysis and Machine Intelligence, Vol. 6, No. 6, pp. 721–741, 1984.

[11] V. Kolmogorov and R. Zabih, “What energy functions can be minimized via graph cuts?” IEEE Transactions on Pattern Analysis and Machine Intelligence, Vol. 26, No. 2, pp. 147–159, 2004.

[12] R. J. Qureshi, L. Kovacs, B. Harangi, B. Nagy, T. Peto, A. Hajdu, “Combining algorithms for automatic detection of optic disc and macula in fundus images”, Computer Vision and Image Understanding, vol. 116, no. 1, pp. 138-145, 2012.

[13] T. Kauppi, V. Kalesnykiene, J. K. Kmrinen, L. Lensu, I. Sorri, A. Raninen, R. Voutilainen, H. Uusitalo, H. Klviinen, and J. Pietil, ”Diaretdb1 diabetic retinopathy database and evaluation protocol”, Medical Image Understanding and Analysis (MIUA 2007), pp. 61-65, 2007.